Geometry Distance Estimated MAC Protocol for TV White Space

Chien-Min Wu and Chih-Pin Lo

***Abstract*—Regulatory bodies worldwide have quite recently approved the dynamic access of unlicensed networks to the TV white space (TVWS) spectrum. In TVWS, secondary users (SUs) are required to access a database periodically to acquire information on the spectrum usage of primary users (PUs). The spectrum database querying of SUs will solve the spectrum scarcity problem. A key technology in efficiently using the TVWS spectrum is designing an efficient medium access control (MAC) protocol. In this paper, we propose a geometry distance estimated medium access control (GMAC) protocol to mitigate the hidden and exposed terminal problems in TVWS. GMAC provides an efficient means of channel database querying to obtain the list of available channels to overcome interference with PUs. We develop a Markov chain model to characterize the saturation normalized throughput of our proposed GMAC protocol for the TVWS. In this study, transmitter power control is based on the geometrically estimated distance between SU communication pairs; this increases channel spatial reuse and throughput, and reduces PU outage probability. We also compare our proposed scheme with existing MAC protocols for TVWS. We show that the GMAC will improve the channel spatial reuse and normalized throughput, and reduce PU outage probability.**

***Index Terms*—Exposed terminal problem, geometry distance estimated, hidden terminal problem, Markov chain model, medium access control (MAC), TV white space (TVWS).**

I. Introduction

CURRENT wireless networks are regulated by a fixed spectrum assignment policy. According to the federal communications commission (FCC), assigned spectrum utilization varies by about 15%–85%, with a high variance in time. In cognitive radio networks (CRNs), secondary users (SUs) perform spectrum sensing to determine the portions of the spectrum that are available [1]–[3]. Spectrum sensing is a key function of CRNs to prevent harmful interference with primary users (PUs) and identify the available spectrum for improving spectrum utilization. However, in practice, the detection performance is often affected with multipath fading, shadowing, and receiver uncertainty [4].

Manuscript received April 5, 2016; revised July 4, 2017 and March 24, 2017; accepted May 3, 2017. Date of publication May 25, 2017; date of current version May 2, 2018. This work was supported by the Ministry of Science and Technology, Taiwan, under Grant MOST 105-2221-E-343-002. *(Corresponding author: Chien-Min Wu.)*

C. M. Wu is with the Department of Computer Science and Information Engineering, Nanhua University, Chiayi 62248, Taiwan (e-mail: cmwu@nhu.edu.tw).

C. P. Lo is with the Department of Computer Science and Information Engineering, National Chung Cheng University, Chiayi 62102, Taiwan (e-mail: ggrobingg@gmail.com).

Digital Object Identifier 10.1109/JSYST.2017.2701802

Several regulatory bodies worldwide have quite recently approved the dynamic access of unlicensed networks to the TV white space (TVWS) spectrum. All existing rules obviated spectrum sensing for the SUs to exploit the TVWS spectrum whenever the spectrum is vacated by PUs. However, the SUs need to access a geographic database periodically for querying the list of TVWS channels free from PUs vacating the channel [5], [6].

Database access for the PUs protection simplifies the access of SUs to the TVWS spectrum, and the research community is actively working on defining several new standards to enable TVWS communication, such as ET Docket 10-174 [7], Ofcom [8], IEEE 802.22 [9], and IEEE 802.11af [10].

The database access of the TVWS spectrum is the first step in solving the spectrum scarcity problem in current wireless networks. However, identifying a mechanism for the efficient use of the TVWS spectrum has become a new challenge. A key aspect in efficiently using the TVWS spectrum is designing an efficient medium access control (MAC) protocol. Therefore, MAC protocols are considerably important to avoid collisions between the SUs and to avoid problems with hidden and exposed terminals in the TVWS [11].

In TVWS, the spectrum can be divided into several channels. A single channel can be used by SUs when there is no interference with other SUs; this improves network performance. In multichannel TVWS, channels are unreliable owing to collisions between SUs and SUs.

The multichannel MAC (MMAC) protocols are an efficient method to solve the contention and collision problems among nodes. MMAC protocols can efficiently improve system throughput, while the maximum throughput of a single-channel MAC protocol is limited by the channel's bandwidth. In addition, multichannel protocols will create fewer propagation delays per channel than a single channel [12].

The hardware limitations of practical cognitive radios are considered in [13]. For the sensing constraint, in a given geometrical area, a spectrum opportunity of interest may span a wide range of bandwidths. For a transmission constraint, the spectrum used by SUs has a maximum bandwidth limit. A decentralized cognitive MAC (DC-MAC) for opportunistic spectrum access in ad hoc networks is proposed in [14]. The authors proposed cognitive MAC protocols that optimize the performance of SUs and avoid the interference with PUs. Without additional control message exchanges between the sender and the receiver of SUs, the proposed distributed protocols ensure synchronous hopping in the spectrum between the sender and the receiver.

An opportunistic spectrum MAC (OS-MAC) for wireless networks equipped with cognitive radios is proposed in [15]. The OS-MAC can adaptively and dynamically seek and exploit opportunities in spectrum access along both the time and frequency dimensions. OS-MAC can efficiently access and share the spectrum among SUs and PUs. In [16], a novel cognitive MAC (C-MAC) protocol for distributed multichannel CRNs is proposed. C-MAC operates under multichannels, and hence is able to efficiently deal with spectrum access among PUs and SUs.

An efficient cognitive-radio-enabled multichannel MAC (CREAM-MAC) protocol for wireless networks is proposed in [17]. In CREAM-MAC, each SU is equipped with a cognitive radio transceiver and multiple channel sensors; as a result, collisions among SUs and between SUs and PUs can be resolved. A MAC protocol for opportunistic spectrum access (OSA-MAC) in CRNs is proposed by [18]. In OSA-MAC, each SU exchange controls information in a dedicated control channel. OSA-MAC uses the power saving mechanism model from IEEE 802.11 DCF-based WLANs.

A novel MAC (N-MAC) scheme adjusts the sensing priorities of channels at each SU with the PU detection information of other SUs and also limits the transmission power of a SU to the maximum allowable power in order to guarantee the quality of the service requirements of the PU [19].

An energy-efficient distributed MMAC protocol is proposed for CR networks [20]. MMAC can achieve energy-efficient communication, and the phases of its sensing algorithms include a low-power inaccurate scan and a high-power accurate scan.

The primary motivation for all of the above MAC protocols is throughput awareness owing to the characteristics of CRNs such as severe resource constraints, hidden terminal problems, and PU outage probability conditions. There is a rising need for efficient throughput-aware MAC protocols proportional to the increasing number of application fields, such as TV white spaces, emergency and public safety applications, vehicular communications, and other novel applications of CRNs [21].

In this paper, we propose a geometry distance estimated MAC (GMAC) protocol for TVWS, to enable SUs to efficiently use the available spectrum. In addition, frequencies reserved for PUs may experience periodic use and frequent quiet periods; thus, SUs may utilize these frequencies during these periods. The SUs can query the channel database to get information of the available spectrum. However, in cases where SUs use PU frequencies, PUs must not be subjected to performance degradation.

These requirements motivated us to design a GMAC protocol for TVWS to overcome the hidden and exposed terminal problems in multichannel TVWS.

The main goal of this paper is to design a GMAC protocol in multihop TVWS. GMAC resolves multichannel hidden terminal problems for SUs, as well as multichannel exposed terminal problems for SUs. The main contributions of this paper are the design of a MMAC protocol for TVWS, and the development of a Markov chain model to characterize the normalized throughput and other performance metrics for the saturation TVWS. In this protocol, requiring two transceivers per node mitigates the hidden and exposed terminal problems in multichannel TVWS, unlike other MMAC protocols that only mitigate the hidden terminal problem.

The remainder of this paper is organized as follows. GMAC protocols are described in Section II. Basic operation of the multichannel GMAC and normalized throughput analysis for the saturation TVWS are described in Sections III and IV, respectively. We evaluate the performance of the proposed GMAC with some numerical results obtained from a simulation in Section V. Finally, this paper concludes in Section VI.

II. GMAC Protocol

In this section, we introduce the GMAC, which enables opportunistic spectrum sharing in TVWS. The GMAC enables significant increases in throughput and channel spatial reuse, and reduces the probability of an outage for PUs. The time structure used is similar to the IEEE 802.11 power-saving mode.

A. System Model in MMAC Protocol TVWS

Several research groups [18], [19], [20], [22]–[25] found the use of a common control channel (CCC) to guarantee reliable control information exchanges for TVWS to be an effective method. However, Ren *et al.* [26] found the use of a dedicated CCC can be expected to cause CCC saturation problems, which often degrades the system performance. Therefore, in our paper, we take the constraint and limits of using the CCC into consideration in the throughput analysis.

We consider a multichannel environment in TVWS. There is one control channel and N data channels within the TVWS. It is assumed that SUs will not be disturbed by PUs in accessing the control channel. The data channels are licensed to PUs and can be opportunistically used by the SUs. In the environment under consideration, the PU and SU signals can have influence not on the entire TVWS but only on part of the TVWS. That is, there exist SUs that cannot detect the PU activation within the TVWS and this will create hidden and exposed terminal problems in TVWS. In addition, the data transmission model is in a multihop environment.

On the other hand, SUs can transmit data traffic with the controlled power by a GMAC as low as possible to avoid influencing PUs. In addition, the SU sender should use minimum power by the GMAC to transmit data traffic to the SU receiver. This will mitigate the hidden and exposed terminal problems for SUs.

Each host has two transceivers to enable it to listen on both the control channel and the data channel simultaneously. Since one of the transceivers is always listening on the control channel, the multichannel hidden terminal problem does not occur [12].

In the proposed GMAC protocol, each SU is equipped with two transceivers: one to communicate with the control channel and one to communicate with data channels. The control transceiver will operate on the control channel to exchange control packets with other SUs and to obtain rights to access data channels. The data transceiver will dynamically

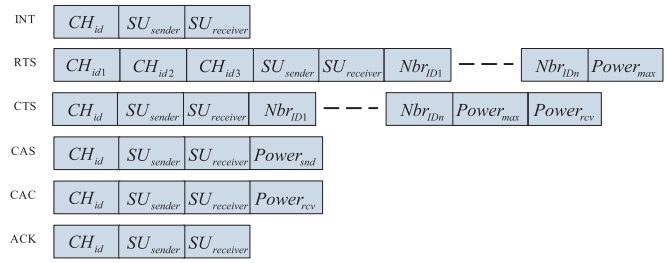

Fig. 1. Control packet for data channel reservation in GMAC protocol of multichannel TVWS.

switch to one of the data channels to transmit data packets and acknowledgements.

B. GMAC Protocol in Multichannel TVWS

In this section, we propose the use of the GMAC protocol in multichannel TVWS to resolve hidden and exposed terminal problems. Before describing the GMAC in detail, we first summarize our assumptions. This protocol uses a scheme similar to [12] that provides throughput improvements using N channels, and all channels have the same bandwidth. None of the channels overlap, thus the packets transmitted on different channels do not interfere with each other. Nodes have prior knowledge regarding the number of available channels. Each node is equipped with two half-duplex transceivers. The transceiver is capable of switching channels dynamically. Nodes are synchronized, allowing them to begin their beacon intervals at the same time.

The GMAC selects the optimum channel based on the channel's condition at the receiver. The protocol achieves throughput improvements by intelligently selecting channels in TVWS. The GMAC operates with one dedicated control channel. At the start of an interval, all nodes must listen to a control channel in order to exchange control packets. During this interval, all nodes can transmit data packets with another transceiver on a data channel.

There are three functions in a GMAC. First, the SU sender and receiver estimate the distance between them and use a deterministic propagation model to determine the transmission power. The SU sender adjusts the transmission range, which decreases interference with the PU. Second, an SU that is in the transmission range of PU_{snd} sends a highest priority interrupt control message to its one-hop neighbors. This will resolve the hidden terminal interference problem for PU_{rcv}. Third, the SU receiver sends a channel confirm control frame to its one-hop neighbors, to resolve the exposed terminal problem for SUs.

In TVWS, the time structure is divided into time intervals, where each interval has two phases. Fig. 2 shows one control channel of the GMAC protocol in multichannel TVWS. The first phase includes a query window, which helps it to avoid PU interference on the same channel. Each SU node maintains a beacon table recording the beacon's probability of success that none of the other nodes transmits in the same beacon slot. The beacon message will return to the backoff mechanism if a collision occurs. Each SU node also maintains a neighbor table, recording its neighbors and including the PUs and SUs.

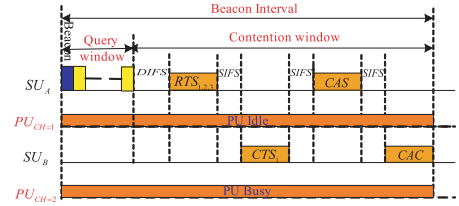

Fig. 2. One control channel in GMAC protocol of multichannel TVWS.

The second phase involves a contention window. In the first phase, the SU node avoids interference with the PU to some extent, but cannot completely avoid it. The second phase will contain the proposed mechanism to resolve the hidden and exposed terminal problems.

The following section contains detailed descriptions of these two phases in a GMAC.

1) Query window phase: Each node sends itself a beacon control message, using the IEEE 802.11 timer synchronization function (TSF) to perform the synchronization. This beacon records its local time in the query window and refreshes its time when it receives a faster beacon time than itself. If a collision occurs between the beacon messages, the backoff mechanism is invoked. IEEE 802.11 and previous documents specify that the SU should change and sense each channel, which is a misuse of energy. In this study, the process of channel database querying obtains the information of available channels.
2) Contention window phase: This phase contains the following control messages: RTS (Request-to-send), CTS (Clear-to-send), PCA (position confirm ACK), CCA (channel confirm assignment), TRC (transmission range confirm), data, and ACK (acknowledgement). Each SU must perform this procedure completely in a control channel before obtaining this channel.

C. Contention Window Descriptions

Fig. 1 shows all the fields of the control packet for data channel reservation in a GMAC protocol of multichannel TVWS. The detailed descriptions are as follows.

1) Beacon: Using IEEE 802.11 TSF.
2) INT: INT contains the following fields: CH_{id}, $\text{SU}_{\text{sender}}$, and $\text{PU}_{\text{sender}}$. CH_{id} denotes the interfered channel to PU, $\text{SU}_{\text{sender}}$ denotes the SUs that sent the interrupt message, and $\text{PU}_{\text{sender}}$ denotes the interfered PU.
3) RTS: The following fields: CH_{id1}, CH_{id2}, CH_{id3}, $\text{SU}_{\text{sender}}$, $\text{SU}_{\text{receiver}}$, $Nbr_{ID1},\cdots,Nbr_{IDn}$ and $\text{Power}_{\text{max}}$ were added to the fields in the CTS of IEEE 802.11. Channels CH_{id1}, CH_{id2}, and CH_{id3} have higher priority in the channel status of the SU sender. $\text{SU}_{\text{sender}}$ denotes the SU sender, $\text{SU}_{\text{receiver}}$ denotes the SU receiver, $Nbr_{ID1},\cdots,Nbr_{IDn}$ denotes the ID of the neighbors of $\text{SU}_{\text{sender}}$, and $\text{Power}_{\text{max}}$ denotes the maximum transmission power of the SU sender.
4) CTS: The following fields: CH_{id}, $\text{SU}_{\text{sender}}$, $\text{SU}_{\text{receiver}}$, $Nbr_{ID1},\cdots,Nbr_{IDn}$, $\text{Power}_{\text{rcv}}$ and $\text{Power}_{\text{max}}$ were added to the fields in the CTS of IEEE 802.11. CH_{id}

denotes the channel selected according to the received RTS message. $\mathrm{SU}_{\mathrm{sender}}$ denotes the SU sender, $\mathrm{SU}_{\mathrm{receiver}}$ denotes the SU receiver, $Nbr_{ID1}, \cdots, Nbr_{IDn}$ denotes the ID of the neighbors of $\mathrm{SU}_{\mathrm{receiver}}$, and $\mathrm{Power}_{\mathrm{rcv}}$ denotes the receiving power of the SU receiver, and $\mathrm{Power}_{\mathrm{max}}$ denotes the maximum transmission power of SU sender.

5) CAS: CAS contains the following fields: CH_{id}, $\mathrm{SU}_{\mathrm{sender}}$, $\mathrm{SU}_{\mathrm{receiver}}$, and $\mathrm{Power}_{\mathrm{snd}}$. CH_{id} denotes the channel selected by the SU sender, $\mathrm{SU}_{\mathrm{sender}}$ denotes the SU sender, $\mathrm{SU}_{\mathrm{receiver}}$ denotes the SU receiver, and $\mathrm{Power}_{\mathrm{snd}}$ denotes the sending power of the SU sender.
6) CAC: CAC contains the following fields: CH_{id}, $\mathrm{SU}_{\mathrm{sender}}$, $\mathrm{SU}_{\mathrm{receiver}}$, and $\mathrm{Power}_{\mathrm{rcv}}$. CH_{id} denotes the channel selected by the SU receiver, $\mathrm{SU}_{\mathrm{sender}}$ denotes the SU sender, $\mathrm{SU}_{\mathrm{receiver}}$ denotes the SU receiver, and $\mathrm{Power}_{\mathrm{rcv}}$ denotes the receiving power of the SU receiver.
7) ACK: ACK contains the following fields: CH_{id}, $\mathrm{SU}_{\mathrm{sender}}$, and $\mathrm{SU}_{\mathrm{receiver}}$. CH_{id} denotes the channel selected by the SU sender, $\mathrm{SU}_{\mathrm{sender}}$ denotes the SU sender, and $\mathrm{SU}_{\mathrm{receiver}}$ denotes SU receiver.

Fig. 2 shows the exchange of control packets and the data channel reserved during the period from the start of the beacon interval to the completion of the contention window. Here, the $\mathrm{PU}_{\mathrm{CH}=1}$ is in the idle state, and $\mathrm{PU}_{\mathrm{CH}=2}$ is in the busy state from the channel database query, respectively. Therefore, SU_A and SU_B select CH_1 as the data communication channel. SU_A estimates the distance to SU_B by a geometrical distance estimated algorithm, and calculates the sending power using the deterministic propagation model.

D. Log-Distance Power-Law Path-Loss Model in Ad Hoc Networks

In [27], the authors proposed a deterministic propagation model for wireless networks. In [28], a shadow fading model for vehicular ad hoc networks is proposed, and a realistic model takes shadowing effects into account with a reasonable amount of complexity. A simple log-distance power law is used to model the path loss that occurs when predicting a reliable communication range between a transmitter and receiver. The log-distance power law path loss model is derived as follows:

$$\mathrm{PL}(d) = \mathrm{PL}_0 + 10n \log_{10}\left(\frac{d}{d_0}\right) + X_\sigma \tag{1}$$

where d is the distance between transmitter and receiver, n is the path loss exponent estimated, and X_σ is zero-mean Gaussian distributed random variable with standard deviation σ. The PL_0 is the path loss at a reference distance d_0 in dB and is based on either close-in measurements or a free space assumption from the transmitter to d_0.

E. Transmit-Power Estimation in GMAC Protocol

Distributed localization algorithms for SUs in cognitive radio ad hoc networks are essential for estimating distance. Geometrical distance estimates rely on the number of shared communication neighbors and applies geometrical properties to the network structure. A geometrical approach provides reliable estimates for the distances between any two adjacent SUs in TVWS [29].

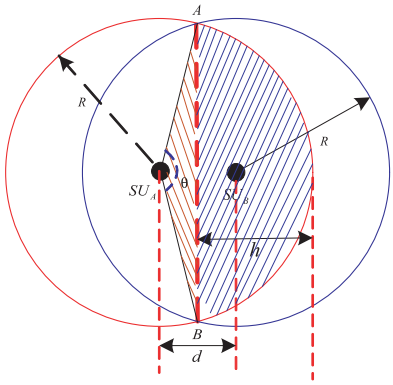

Fig. 3. Estimation of the overlapping surface of the communication area of two adjacent SUs.

The basic idea of geometrical distance estimation is to approximately determine the common surface of two overlapping communication areas by the ratio of shared to total neighbors. Knowing the overlapping surface, the distance between the two communicating SUs can be derived. The distance can then be used as input for the power estimation [29].

Fig. 3 shows how to estimate the overlapping surface of the communication area of two adjacent SUs. The requirements for the geometrical distance estimation algorithm are that each SU knows all its neighbors and can communicate with them.

For SU_A, the sector area (the sum of the red-dotted-line area and blue-solid-line area) of points SU_A, A, and B, is

$$S_{\mathrm{SU}_A AB} = \pi R^2 * \frac{\theta}{2\pi} = \frac{1}{2}R^2\theta. \tag{2}$$

The triangular area (the-red-dotted line area) of points, SU_A, A, and B, is

$$\triangle_{\mathrm{SU}_A AB} = \frac{1}{2} * \frac{d}{2} * 2R\sin\frac{\theta}{2} = \frac{1}{2}dR\sin\frac{\theta}{2}. \tag{3}$$

The network structure of two adjacent SUs and their communication area can be mapped to the geometrical shape of two overlapping circles. The problem of determining the distance between the adjacent SUs becomes a computation of the distance between the corresponding circles' centers. The surface of the overlapping area OA can be estimated as follows:

$$\begin{aligned} OA &= 2 * (S_{\mathrm{SU}_A AB} - \triangle_{\mathrm{SU}_A AB}) \\ &= 2 * \left(\frac{1}{2}R^2\theta - \frac{1}{2}dR\sin\frac{\theta}{2}\right) \\ &= R^2\theta - dR\sin\frac{\theta}{2}. \end{aligned} \tag{4}$$

For $\triangle_{\mathrm{SU}_A AB}$, $\cos\frac{\theta}{2} = \frac{\frac{d}{2}}{R} = \frac{d}{2R}$,
therefore $\theta = 2\cos^{-1}(\frac{d}{2R})$, and $\sin\frac{\theta}{2} = \sqrt{1 - \frac{d^2}{4R^2}}$,

$$OA = 2R^2\cos^{-1}\left(\frac{d}{2R}\right) - \frac{1}{2}d\sqrt{4R^2 - d^2}. \tag{5}$$

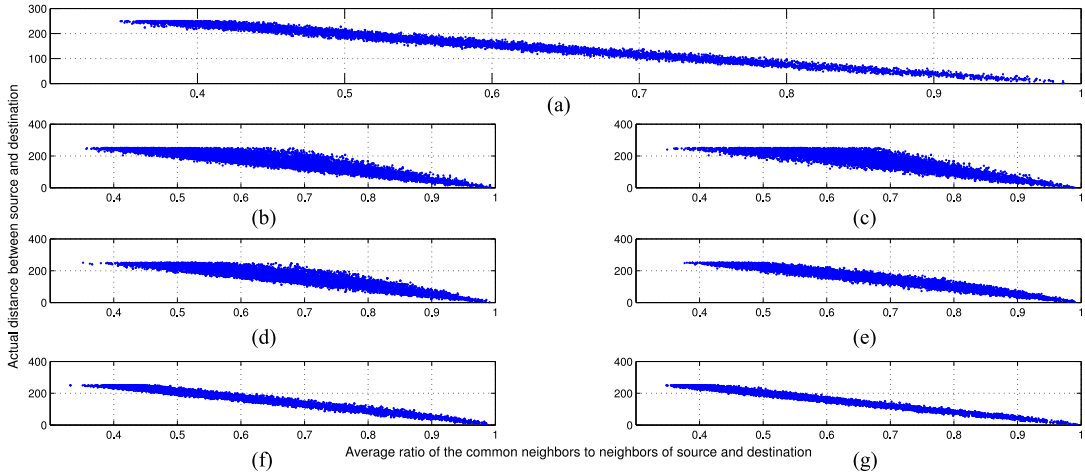

Fig. 4. Actual distance between source and destination versus average ratio, which is the common neighbors to neighbors of source and destination. (a) more than 250 m from the border.

From the relations among d, h, and R, the distance between the two centers can be obtained by $d = 2(R - h)$.

Therefore, the overlapping surface OA can be calculated from an unknown distance between SU_A and SU_B and a segment height h

$$OA = 2R^2 \cos^{-1}\left(1 - \frac{h}{R}\right) - 2(R-h)\sqrt{2Rh - h^2}. \quad (6)$$

As (6) depends on h and R, there is no two-dimensional representation that can be approximated by using regression. Nevertheless, the following considerations help to solve this problem. The height h of a segment can be described as a ratio α of the circle's radius R, and the segment area OA is a portion of half the circle's surface [29], and we can get $\alpha = \frac{h}{R}, \beta = \frac{OA}{\pi R^2}$.

Here, we show that α and β are independent of R, with the result that the relationship between α and β can be approximated using regression. Because $\cos\frac{\theta}{2} = \frac{\frac{d}{2}}{R} = \frac{1}{R} = 1 - \frac{h}{R}$,

Therefore, $h = R(1 - \cos\frac{\theta}{2})$, and we can get

$$\alpha = \frac{h}{R} = 1 - \cos\frac{\theta}{2} \quad (7)$$

$$\beta = \frac{OA}{\pi}R^2 = \frac{1}{\pi}R^2\left(R^2\theta - dR\sin\frac{\theta}{2}\right) = \frac{1}{\pi}\left(\theta - \frac{d}{R}\sin\frac{\theta}{2}\right). \quad (8)$$

So,

$$\begin{aligned}\beta &= \frac{1}{\pi}\left(\theta - 2\frac{\frac{d}{2}}{R}\sin\frac{\theta}{2}\right)\\ &= \frac{1}{\pi}\left(\theta - 2\cos\frac{\theta}{2}\sin\frac{\theta}{2}\right)\\ &= \frac{1}{\pi}\left(\theta - \sin\theta\right). \end{aligned} \quad (9)$$

From above, we show that α and β are independent of R.

In [29], the authors showed that the optimal distance can be obtained by a third-degree polynomial function:

$$d_{AB} = R\left(a * \left(\frac{N_{AB}}{N_{\mathrm{SU}_A}}\right)^3 + b * \left(\frac{N_{AB}}{N_{\mathrm{SU}_A}}\right)^2 + c * \left(\frac{N_{AB}}{N_{\mathrm{SU}_A}}\right) + e\right) \quad (10)$$

$$d_{BA} = R\left(a * \left(\frac{N_{BA}}{N_{\mathrm{SU}_B}}\right)^3 + b * \left(\frac{N_{BA}}{N_{\mathrm{SU}_B}}\right)^2 + c * \left(\frac{N_{BA}}{N_{\mathrm{SU}_B}}\right) + e\right). \quad (11)$$

Then the estimated distance d between SU_A and SU_B is

$$d = \frac{1}{2}(d_{AB} + d_{BA}). \quad (12)$$

Fig. 4 shows the average ratio of the common neighbors to the neighbors of source and destination versus the actual distance between source and destination. Fig. 4 shows the 10 000 connections that are created by random selection of one source and destination in 1200 nodes within a bounded region of 1200×1200 m^2. Fig. 4(a)−(g) shows the selected nodes that are more than 250, 0−250, 0−50, 50−100, 100−150, 150−200, and 200−250 m from the border, respectively. As nodes near the border of the network have a cropped communication area, the average estimation error will increase. Thus as the selected communication pairs that have the selected nodes near the border of the network increase, the estimation error increases.

In the actual environment, the distance from the border for each node is unknown. Any node cannot know the location of the border. In this paper, four points are selected for each time from Fig. 4(a) to estimate the errors in Fig. 10 under different conditions. In Fig. 5(a)−(g), the estimation errors 5.06%, 19.26%, 23.14%, 20.75%, 15.47%, 8.33%, and 5.69%, respectively.

Using regression to determine the polynomials d_{AB} and d_{BA} and further computations, the coefficients of the above

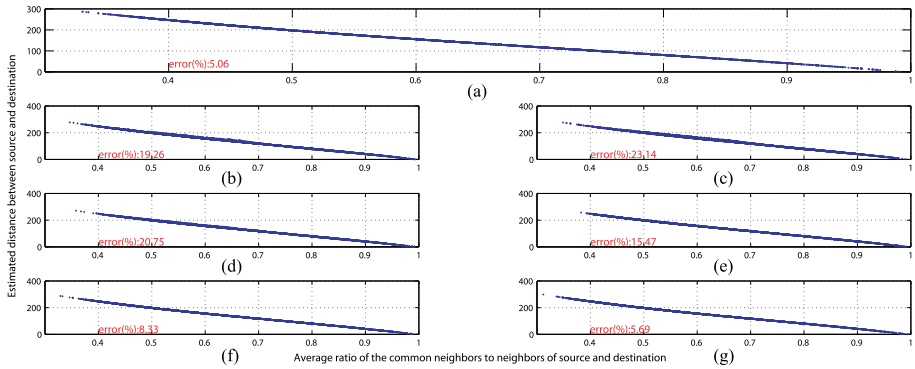

Fig. 5. Estimate distance between source and destination versus average ratio, which is the common neighbors to neighbors of source and destination. (a) more than 250 m from the border.

equation can be estimated as follows: $a = -1.992, b = 4.394, c = -4.707$, and $e = 2.294$.

III. Basic Operation in Multichannel GMAC

Each SU determines channel vacancy based only on its querying outcomes. The SU should perform spectrum querying to obtain the list of available channels. Each SU maintains various state data for each channel.

A. Channel State Information in Multichannel GMAC

The data for channel i at node j is as follows.

1) $\mathrm{CH}_i(j)$: This denotes the state of channel i at $\mathrm{SU}(j)$. Let $\mathrm{SU}(i)$ denote a cognitive radio secondary user i, and $\mathrm{PU}(j)$ denote a primary user j. If $\mathrm{SU}(j)$ detects other SU signals on channel i in the contention window, it sets $\mathrm{CH}_i(j) = 1$. Otherwise, $\mathrm{CH}_i(j) = 0$. When $\mathrm{CH}_i(j) = 0$, $\mathrm{SU}(j)$ considers channel i to be empty.
2) $\mathrm{PU}_i(j)$: This indicates the $\mathrm{SU}(j)$ that has obtained the information of the existence of a PU on channel i from the channel database querying in the query window. If the $\mathrm{SU}(j)$ verifies the existence of the PU on the channel i, it sets $\mathrm{PU}_i(j) = 1$. Otherwise, $\mathrm{PU}_i(j) = 0$. When $\mathrm{PU}_i(j) = 0$, the $\mathrm{SU}(j)$ considers the channel i to be empty.

B. Channel Database Querying in Query Window

In GMAC, periodically transmitted beacons divide time into beacon intervals. A small window on the control channel, called the query window, is placed at the start of each beacon interval. During this window, each SU may query the channel database to obtain a list of available channels. Each SU records querying data channels whether they are occupied by PUs.

C. Data Transmission Scheme in Multichannel GMAC

In the query window, each SU queries and obtains a list of available channels. The contention window is used for control packet exchanges and selects one idle channel. In the contention window, the transmission range of the SUs on the data channels cannot cover the entire network, because the SUs transmit data packets using power controlled by GMAC. Thus, some $\mathrm{SU}_{\mathrm{sender}}$ and $\mathrm{SU}_{\mathrm{receiver}}$ pairs in the TVWS will use multihop data transmissions. A multihop transmission is composed of several concatenated one-hop transmissions; a proposed data transmission scheme governs each one-hop transmission, where the $\mathrm{SU}_{\mathrm{receiver}}$ is located within the transmission range of the $\mathrm{SU}_{\mathrm{sender}}$ [19]. An $\mathrm{SU}_{\mathrm{sender}}$ that wants to transmit data packets should first reserve a data channel. Data channels are reserved by an exchange of control packets between an SU_{sender} and SU_{receiver}. In GMAC, packet transmissions on the control channel are governed by a modified IEEE 802.11, referred to as GMAC.

GMAC is designed to solve multichannel hidden and exposed terminal problems. The GMAC procedures for resolving multichannel hidden terminal problems are performed as follows.

1) Upon receiving a beacon at the query window, each SU obtains the PUs' idle channel information from the query window. If $\mathrm{SU}(i)$ obtains the information of an available PU_c channel, it sets $\mathrm{PU}_c(i) = 1$. Otherwise, $\mathrm{PU}_c(i) = 0$. The notation c denotes licensed channels. In this scenario, c ranges from 1 to 4.
2) If $\mathrm{SU}(i)$ has a data packet to send to $\mathrm{SU}(j)$, then $\mathrm{SU}(j)$ is also a cognitive radio secondary user j.
3) SU_i obtains the status of $\mathrm{PU}_c(i)$ for each licensed channel of the PU by querying the channel database. SU_i selects the idle channels from $\mathrm{PU}_c(i)$ and then selects three channels (CH_{id1}, CH_{id2}, and CH_{id3}) that have higher probabilities of success from the channel status table. It then adds the selected channels, the ID of the one-hop neighbors of SU_i and the maximum transmission power information, $\mathrm{Power}_{\mathrm{max}}$, to the RTS control packet in the contention window, and sends it to SU_j. Here, it is assumed that all the SUs have the same maximum transmission power, $\mathrm{Power}_{\mathrm{max}}$.
4) Assume SU_j receives the RTS control message from SU_i, and then selects one channel, CH_{id}, according to the success probability data in its channel status table and whether the status $\mathrm{PU}_c(j)$ is 0. SU_j then sends the CTS control message, including the selected channel CH_{id}, and the ID of the one-hop neighbors of SU_j to SU_i after waiting the short interframe space (SIFS) time interval. The CTS also includes the receiving power, $\mathrm{Power}_{\mathrm{rcv}}$, of the SU_j to SU_i transmission, and the maximum transmission power $\mathrm{Power}_{\mathrm{max}}$, of SU_j. If SU_j has no suitable $\mathrm{PU}_c(j)$ channel in its status stable, the channel field CH_{id} of CTS

is set to empty. As a result, the connection cannot be established and SU(i) must wait for the next frame; the above procedures are repeated if SU(i) still wants to establish communication between SU(i) and SU(j).

5) SU_i calculates the common neighbors from the received neighbors' ID of SU_j. SU_i estimates distance to SU_j by geometry distance estimated algorithm and calculates the sending power using the deterministic propagation model, adds this information to the CAS, and sends it to SU_j. If the estimated distance is larger than 250 m, the distance between SU_i and SU_j is set to the maximum transmission range of 250 m.
6) The transmission power of SU_i is adjusted to minimum power $\text{Power}_{\text{min}}(i)$ before sending the transmission to SU_j. Therefore, the interference range of SU_i must be reduced. Then, the hidden terminal interference problems of the communication between SU_i and SU_j will be mitigated for the PU and SU.
7) SU_j sends the CAC control packet to SU_i. When the estimated distance is lower than the actual distance, SU_i cannot receive the CAC control packet from SU_j, and the process moves on to the next beacon interval cycle to repeat the GMAC procedure. Fig. 5 shows the estimated distance error of the GMAC ranged from 5.06% to 23.14%. Therefore, if the estimated distance is lower than the actual distance, 6% estimation error is added to the estimated distance, and the process is repeated up to four times. If the problem remains unsolved, GMAC is terminated.
8) Assume a PU receiver is receiving a transmission from a PU sender. In addition, the PU receiver remains in the transmission range of SU_i after the power is adjusted. If one cognitive radio node SU_C is in the transmission range of SU_i and the PU sender, SU_C will send the interrupt message INT to the one-hop neighbors of SU_C. Then, to avoid interference with the PU, the communication between SU_i and SU_j can be terminated or moved to another channel. As a result, the hidden terminal interference problem of the PU receiver will be successfully resolved at least mitigated. If there are no SUs in the transmission range of SU_i and the PU sender, the hidden terminal problem will only be mitigated by querying a channel in the query window and reducing the transmission range.
9) In addition, the exposed terminal problem will be mitigated by reducing the transmission range and querying the channels in the query window.

D. Channel Assignment in Multichannel GMAC

In [30] and [31], the authors proposed two channel assignment schemes: the nonoverlapped and overlapped channel assignments. For a nonoverlapped channel assignment, each SU is assigned to different channels. The maximum throughput will be achieved if the number of data channels is sufficiently large. However, we never have a very large number of channels to support each SU in the nonoverlapped channel assignment. In contrast, for the overlapped channel assignment, a MAC protocol is necessary to resolve the contention when several SUs attempt to access the same assigned channel. In addition, a channel spatial reuse of the overlapped channel is necessary to improve the network throughput.

Suppose there is a pool of *M* channels available to the network, and they are numbered from 1 to *M*. Let

$$\text{CH}_{\text{one}}(i,j) = \begin{cases} 1, & \text{channel } i \text{ is used at node } j \\ 0, & \text{otherwise} \end{cases}$$

$$\text{CH}_{\text{mul}}(i) = \begin{cases} 1, & \text{channel } i \text{ is used at least one node} \\ 0, & \text{otherwise.} \end{cases}$$

When an SU sender requests to set up a connection with a destination SU, the SUs will run the MAC protocol of the GMAC to mitigate the multichannel hidden terminal problem and then access one usable channel by the channel assignment of the GMAC. If a channel i is used at node j, the SU then updates its $\text{CH}_{\text{one}}(i,j)$. Other SUs can update their $\text{CH}_{\text{mul}}(i)$ by exchanging or receiving control packets RTS/CTS/CAS/CAC of the GMAC.

To increase the channel spatial reuse, when there is no risk of violating the hidden terminal problem constraints, effort should be taken to reuse the assigned channel as often as possible. Since an exchange of control packets keeps track of the usage status of each channel, the GMAC system assumes a compact pattern for channel spatial reuse. However, the SUs then have to exchange the channel status information by exchanging control packets, resulting in a higher control traffic load.

IV. Throughput Analysis for the Saturation Network

An interference model for one PU and multiple SUs under a primary signal-to-interference-plus-noise (SINR) constraint is proposed [24]. The desired signal (transmitted by PU_{snd}, and received by PU_{rcv}) and the interference signal (transmitted by SU_{snd}, and intended for SU_{rcv}) are subject to Rayleigh fading and path loss. The interference control scheme considered for dynamic spectrum access allows PU and SUs to share the same band, provided that the SINR required by the PU (denoted SINR_{th}) is attained. The arrival traffic rates of the PU and SUs are assumed to be Poisson processes denoted by λ_P and λ_S, respectively. The departure traffic rate of the PUs and SUs are modeled with Poisson processes with rates of μ_P and μ_S, respectively.

The PU can transmit data packets when its SINR is greater than SINR_{th}. Otherwise, the SUs may transmit data packets on this band if this constraint cannot be satisfied. In addition, PUs and SUs can coexist if the primary SINR is greater than SINR_{th}. Finally, if a PU is able to transmit, and coexistence with an SU is not possible because of the SINR constraint, the SUs will be silent.

P_{fail} represents the probability that a PU sender is not able to transmit data packets because of poor channel quality, even in the absence of SUs. P_{share} represents the probability that a PU sender can transmit data packets and coexist with SUs to share a channel. P_{suc} represents the probability that a PU can use the channel and cannot share it with SUs [24]. Here, $P_{\text{fail}} = \text{Prob}(\text{SINR}_{\text{PU}_{\text{interference}=0}} < \text{SINR}_{\text{th}})$, $P_{\text{share}} = \text{Prob}(\text{SINR}_{\text{PU}} > \text{SINR}_{\text{th}})$, and $P_{\text{suc}} = 1 - P_{\text{share}} = \text{Prob}(\text{SINR}_{\text{PU}} \leq \text{SINR}_{\text{th}})$.

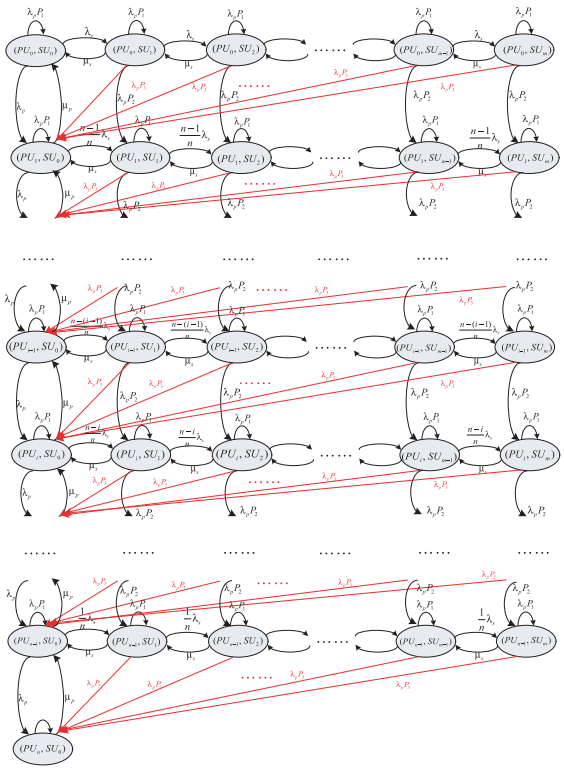

Fig. 6. Markov chain modeling interference control with multiple PUs and multiple SUs.

In Fig. 6, continuous-time Markov Chain models a GMAC system containing multiple PUs and SUs. GMAC assumes that each PU channel is independent, and that the PU channels do not overlap. The different states are as follows.

1) $(\mathrm{PU}_0, \mathrm{SU}_0)$: There are no transmissions by any PUs or SUs. The number of PUs and SUs is 0.
2) $(\mathrm{PU}_0, \mathrm{SU}_j)$: Only the SUs are transmitting. The numbers of PUs and SUs are 0 and j, respectively.
3) $(\mathrm{PU}_i, \mathrm{SU}_0)$: Only the PUs are transmitting. The numbers of PUs and SUs are i and 0, respectively.
4) $(\mathrm{PU}_i, \mathrm{SU}_j)$: The numbers of PUs and SUs are i and j, respectively. The PUs and SUs can coexist to share the channel.

The analysis of the GMAC system is illustrated in Fig. 6; please see the Appendix.

A performance analysis of the IEEE 802.11 DCF in wireless LAN is proposed in [32]. The saturation throughput by analyzing the licensed data channels is derived in [17] and the normalized saturation throughput by analyzing the licensed data channels is derived in [25]. γ is defined as the channel utilization under PU ON and OFF states for all licensed channels. We assumed that all the licensed channels had the same channel utilization.

For n licensed data channels, the probability that there will be i vacant PU channels is

$$P_{\mathrm{VC}}(i) = \sum_{j=1}^{m} \pi_{(i,j)} = \binom{n}{i} (1-\gamma)^i \gamma^{n-i}. \tag{13}$$

The average number of vacant channels that can be used by SUs can be derived by

$$\begin{aligned} E[\mathrm{CH}_{\mathrm{vacant}}] &= \sum_{i=1}^{n}\sum_{j=1}^{m} i\pi_{(i,j)} \\ &= \sum_{i=1}^{n} iP_{\mathrm{VC}}(i) \\ &= \sum_{i=1}^{n} i \binom{n}{i} (1-\gamma)^i \gamma^{n-i} \\ &= n(1-\gamma). \end{aligned} \tag{14}$$

We evaluated GMACs performance in TVWS, based on the following metrics:

1) Channel spatial reuse index η: The average number of times that a channel is being used simultaneously. It is defined as follows:

$$\eta = \frac{\sum_{i=1}^{M}\sum_{j=1}^{N} \mathrm{CH}_{\mathrm{one}}(i,j)}{\sum_{i=1}^{M} \mathrm{CH}_{\mathrm{mul}}(i)}. \tag{15}$$

2) Normalized throughput ζ: the normalized throughput under overload condition of the multichannel TVWS. In TVWS, PUs use licensed channels dynamically; the licensed channels used by SUs are alternated between ON and OFF states. The normalized throughput of the multichannel TVWS ζ (with n licensed data channels, and one control channel) is defined as follows:

$$\zeta = \frac{\eta R_{\mathrm{data}} E[\mathrm{CH}_{\mathrm{vacant}}] E[T]}{(nR_{\mathrm{data}} + R_{\mathrm{control}})(E[T] + nT_{\mathrm{ms}})} \tag{16}$$

where R_{data} is the data rate of a licensed channel, R_{control} is the data rate of a control channel, T_{ms} is the mini-slot time units in query window, $E[\mathrm{CH}_{\mathrm{vacant}}]$ is the average number of vacant channels, and $E[T]$ is the average time that is required for the successful handshakes of RTS/CTS/CAS/CAC of GMAC. There is a detailed analysis of $E[T]$ in Appendix.

V. Performance Evaluation

In this section, we present the simulation results for the performance evaluation of the protocols. The simulation is based on event-driven programming and implemented in C programming language. The main difference between the GMAC and MMAC system is the traffic scenario. In the multihop scenario, the MMAC system generates only two traffic streams that cross the network diagonally [20]. In this paper, the traffic is assumed to be uniformly distributed among all nodes with various overall loads (or erlangs, the ratio of the arrival rate to the departure rate) for GMAC and MMAC. In MMAC, there was a factor of more than five gain in throughput for the best case presented (five data channels, no PU activity). In addition, one transceiver is needed in [20], two transceivers is necessary in GMAC. Therefore, we compare GMAC's performance with that of the MMAC scheme, where channels are assigned to a connection on demand.

The cognitive radio ad hoc network is simulated by placing 400 nodes randomly within a bounded region of 1200 $\times$

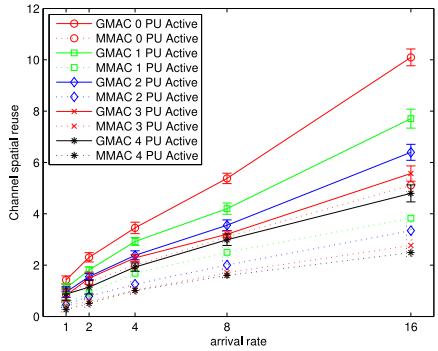

Fig. 7. Comparison of channel spatial reuse of GMAC and MMAC versus arrival rate a channel in multichannel TVWS.

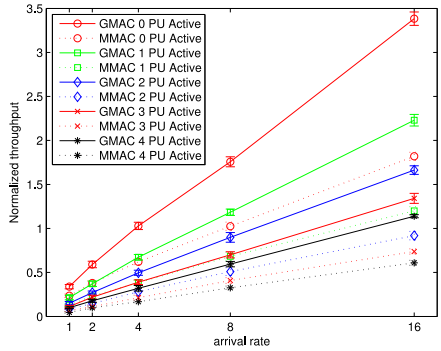

Fig. 8. Comparison of normalized throughput of GMAC and MMAC versus arrival rate on a channel in multichannel TVWS.

1200 m^2. It is assumed that nodes will be continuously powered ON. Before the transmission range is adjusted for each node, the control message transmission range for SUs is fixed at 250 m; each simulation runs for 20 000 s. The transmission range for PUs is fixed at 300 m. There are four PUs, placed at (300, 300), (900, 300), (300, 900), and (900, 900). There are four data channels. Each PU has its own channel and not overlap in the transmission range. The transmission rates for each data channel is 2 Mb/s and the transmission rate for control channel is 1 Mb/s. The sizes of RTS, CTS, CAS, and CAC packets are given as 125, 125, 15, and 21 bytes, respectively. In addition, T_{ms}, SIFS, and DCF interframe space (DIFS) are given as 9 μs, 15 μs, and 34 μs, respectively. The state of a channel alternates between the PU ON state, where a PU is busy on the channel and the PU OFF state, where the channel is idle for a PU. The PU ON duration of each channel are exponentially distributed with mean 300 s. We do not consider mobility in this paper, and all nodes are assumed to be stationary to eliminate the effects of broken routes caused by mobility.

Each of our simulation results is the average of ten randomly generated network topologies, each with a different seed. All reported results were averaged over ten seeds. Furthermore, to generate a more uniform topology, we divided the topology into 100 regions and randomly dispersed the 400 SUs in the regions. This prevented the network from becoming disconnected when N (the average number of neighbors) was small. The distances between the source node and the destination node were also uniformly distributed. That is, we ensured that there were roughly equal numbers of short, medium, and long connections.

The arrival rate is the number of newly arriving connections per second. The departure rate is the number of terminated connections per second, and is also the inverse of the average lifetime of a connection. To obtain the desired traffic load, the departure rate was fixed at 0.05 and the arrival rate was 1, 2, 4, 8, and 16. Therefore, when the arrival rate was 16, the overall load was 320, indicating that there were 320 active connections in the network, on average. For a given traffic load (arrival rate), we first determine when a new connection request should arrive. Subsequently, its source and destination are determined independently from the uniform distributions. Therefore, the number of connection requests depends on the load, but not on the number of nodes.

Fig. 7 shows the channel spatial reuse index η for GMAC and MMAC with a 99% confidence interval versus the arrival rate for a channel in multichannel TVWS. For GMAC, the channel spatial reuse index η can be higher than 1.0 because channels are reused if no interference problems can occur. GMAC produces the highest channel spatial reuse, because it adjusts the transmission range and reduces the interference range of PUs and SUs. We observe that the channel spatial reuse of GMAC ranged from 0.95 (arrival rate $=1$) to 6.39 (arrival rate $=16$) for different arrival rate on a channel (for two channels active of PU ON). For MMAC, the channel spatial reuse ranged from 0.46 (arrival rate $=1$) to 3.34 (arrival rate $=16$) for different arrival rate on a channel (for two channels active of PU ON). The channel spatial reuse improvements for GMAC compared to MMAC raged from 51.6% to 47.7%. For GMAC, as the arrival rate for a channel increases, the channel spatial reuse increases; as the PU activity ratio increases, the channel spatial reuse decreases.

Fig. 8 shows the normalized throughput index ζ for GMAC and MMAC with a 99% confidence interval versus the arrival rate for a channel in multichannel TVWS. We observe that the normalized throughput of GMAC ranged from 0.15 (arrival rate $=1$) to 1.66 (arrival rate $=16$) for different arrival rates on a channel (for two channels active of PU ON). For MMAC, the normalized throughput ranged from 0.08 (arrival rate $=1$) to 0.92 (arrival rate $=16$) for different arrival rates on a channel (for two channels active of PU ON). The normalized throughput improvements for GMAC compared to MMAC raged from 46.7% to 44.6%. For GMAC, as the channel active of PU ON decreases, the normalized throughput increases, but the required arrival rate on a channel increases to achieve the maximum normalized throughput. In this paper, the normalized throughput of GMAC is defined in (16), and the channel spatial reuse is included in the numerator of (16). From Fig. 7, the channel spatial reuse is higher than 1.0. Hence, the maximum normalized throughput is also greater than 1.0.

Fig. 9 shows the influence that PU activation/deactivation frequency has on the PU outage probability with a 99% confidence interval. In MMAC, interference to a PU is avoided by enabling SUs in the transmission range of the PU to notify the communication pairs that may interfere with the PU. For GMAC, the SU in the transmission range will inform the one-hop neighbors, which will reduce the probability of an outage. Despite reductions in channel spatial reuse and throughput in this method, GMAC still provides higher spatial channel reuse and normalized throughput by determining power control according to estimated distance. Fig. 9, shows that the outage

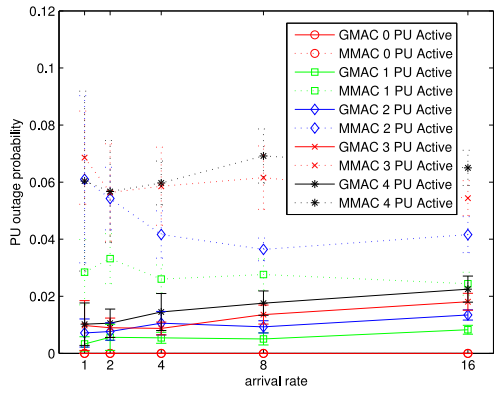

Fig. 9. Comparison of PU outage probability of GMAC and MMAC versus arrival rate on a channel in multichannel TVWS.

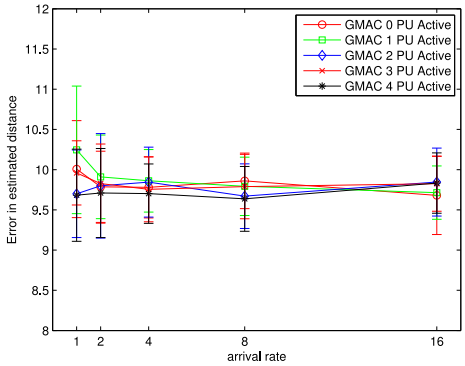

Fig. 10. Errors in estimated distance of GMAC versus arrival rate on a channel in multichannel TVWS.

probability of GMAC ranges from 0.7% (arrival rate = 1) to 1.3% (arrival rate = 16) for different arrival rates on a channel (for two channels active of PU ON). For MMAC, the outage probability of MMAC ranges from 6.1% to 4.2% for different arrival rates on a channel (for two channels active of PU ON). The outage probability improvement provided by GMAC compared to MMAC ranged from 88.52% to 69.04%. In GMAC, as the arrival rate on a channel increases, the outage probability increases; as the PU activity ratio increases, the outage probability increases. Because the power control mechanism can reduce the mutual interferences among the PUs and SUs, it can efficiently reduce the PU outage probability and significantly increase the network throughput. Therefore, the power control mechanism of the GMAC system will have a higher channel spatial reuse and normalized throughput, and a lower PU outage probability than MMAC does, as the later has no power control mechanism.

Fig. 10 shows the average error in the GMAC's estimated distance with a 99% confidence interval versus the PU activation/deactivation frequency. As shown in the figure, the estimation error of the GMAC system ranges from 9.31% to 9.79% (for two channels active of PU ON). The estimation error will increase if the SUs near the border of the network have a cropped communication area. In contrast, the average estimation error will decrease when the SUs near the center keep away the border of the network.

In the actual environment, the distance from the border for each node is unknown. Any node cannot know the location of the border.

In MMAC, SU sender transmits a data packet using the fixed power, which is equal to the maximum allowable transmission power, and the interference to a PU is avoided by enabling SUs in the transmission range of the PU to notify the communication pairs that may interfere with the PU. For GMAC, the SU in the transmission range will also inform the one-hop neighbors, which will reduce the probability of an outage, and the SUs having data packets first select the data channels according to the channel's probability of success and then it transmits the packets with the optimum transmission power. Therefore, GMAC provides higher spatial channel reuse and normalized throughput by determining power control according to estimated distance, and also provides the lower PU outage probability.

VI. Conclusion

We have proposed an efficient MAC protocol based on channel database querying for multichannel TVWS. We showed that a geometrical distance estimation results in significant improvements to transmission power estimation. The proposed method, referred to as the GMAC protocol in multichannel TVWS, will mitigate the hidden and exposed terminal problems for PUs and SUs by estimating geometrical distance to adjust the transmission range. In a GMAC, by estimating the distance between SUs and controlling the transmission power of packets to guarantee the quality of service requirements of PUs. The proposed GMAC scheme effectively protects not only the hidden terminal PUs and SUs but also mitigates the exposed terminal problems between SUs. Therefore, the GMAC provides for higher spatial channel reuse, normalized throughput, and lower PU outage probability. The simulation results show that the outage probability was reduced from 88.52% to 69.04% (for two channels active of PU ON). In addition, the GMAC determines power control according to estimated distance, to obtain improved channel spatial reuse and normalized throughput. As shown in the simulation results, channel spatial reuse improved from 51.6% to 47.7% and normalized throughput improved from 46.7% to 44.6% (for two channels active of PU ON).

Appendix

The analysis of the GMAC system is illustrated in Fig. 6 consists of the following equation systems:

$$\begin{cases} \pi_{0,0} + \cdots + \pi_{0,m} + \cdots + \pi_{n,0} + \cdots + \pi_{n,m} = 1 \\ \pi_{1,0}\mu_p + \pi_{0,1}\mu_s = \pi_{0,0}(\lambda_p + \lambda_s) \\ \pi_{0,j-1}\lambda_s + \pi_{0,j+1}\mu_s = \pi_{0,j}\alpha_1 \\ \pi_{0,m-1}\lambda_s = \pi_{0,m}\alpha_2 \\ \pi_{i-1,0}\lambda_p + \pi_{i+1,0}\mu_p + \pi_{i,1}\mu_s + \lambda_p P_{\text{suc}}\beta_1 = \pi_{i,0}\alpha_3 \\ \pi_{i-1,j}\lambda_p P_{\text{share}} + \pi_{i,j-1}\frac{n-i}{n}\lambda_s + \pi_{i,j+1}\mu_s = \pi_{i,j}\alpha_4 \\ \pi_{i-1,m}\lambda_p P_{\text{share}} + \pi_{i,m-1}\frac{n-i}{n}\lambda_s = \pi_{i,m}\alpha_2 \\ \pi_{n-2,0}\lambda_p + \pi_{n,0}\mu_p + \pi_{n-1,1}\mu_s + \lambda_p P_{\text{suc}}\beta = \pi_{n-1,0}\alpha_5 \\ \pi_{n-2,j}\lambda_p P_{\text{share}} + \pi_{n-1,j-1}\frac{1}{n}\lambda_s + \pi_{n-1,j+1}\mu_s = \pi_{n-1,j}\alpha_6 \\ \pi_{n-2,m}\lambda_p P_{\text{share}} + \pi_{n-1,m-1}\frac{1}{n}\lambda_s = \pi_{n-1,m}\alpha_7 \\ \pi_{n-1,0}\lambda_p + \lambda_p P_{\text{suc}}\beta_3 = \pi_{n,0}\mu_p \\ i = 1, \ldots, n-2 \\ j = 1, \ldots, m-1 \end{cases} \quad (17)$$

$$\begin{bmatrix}
1 & 1 & \cdots & 1 & 1 & 1 & \cdots & 1 & 1 & 1 & \cdots & 1 & 1 & 1 & \cdots & 1 & 1 & 1 \\
-\alpha_1 & \mu_s & \cdots & 0 & 0 & 0 & \cdots & 0 & 0 & \mu_p & \cdots & 0 & 0 & 0 & \cdots & 0 & 0 & 0 \\
0 & 0 & \cdots & -\lambda_s & -\alpha_1 & \mu_s & \cdots & 0 & 0 & 0 & \cdots & 0 & 0 & 0 & & & & \\
0 & 0 & \cdots & 0 & 0 & 0 & \cdots & \lambda_s & -\alpha_2 & 0 & \cdots & 0 & 0 & 0 & \cdots & 0 & 0 & 0 \\
\cdots & & \cdots & & & & \cdots & & & & \cdots & & & & & & & \cdots \\
\vdots & & \vdots & & & & \vdots & & & & \vdots & & \vdots & & & & & \vdots \\
\cdots & & \cdots & & & & \cdots & & & & \cdots & & \cdots & & & & & \cdots \\
0 & 0 & \cdots & 0 & 0 & 0 & \cdots & \cdots & 0 & 0 & \cdots & 0 & \lambda_p & \lambda_p P_3 & \cdots & 0 & \lambda_p P_3 & -\mu_p
\end{bmatrix} \tag{18}$$

with

$\beta_1 = \pi_{i-1,1} + \cdots + \pi_{i-1,m}$
$\beta_2 = \pi_{n-2,1} + \cdots + \pi_{n-2,m}$
$\beta_3 = \pi_{n-1,1} + \cdots + \pi_{n-1,m}$
$\alpha_1 = \lambda_p P_{\text{share}} + \lambda_p P_{\text{suc}} + \mu_s + \lambda_s$
$\alpha_2 = \lambda_p P_{\text{share}} + \lambda_p P_{\text{suc}} + \mu_s$
$\alpha_3 = \mu_p + \lambda_p + \frac{n-i}{n}\lambda_s$
$\alpha_4 = \lambda_p P_{\text{share}} + \lambda_p P_{\text{suc}} + \mu_s + \frac{n-i}{n}\lambda_s$
$\alpha_5 = \mu_p + \lambda_p + \frac{1}{n}\lambda_s$
$\alpha_6 = \lambda_p P_{\text{suc}} + \mu_s + \frac{1}{n}\lambda_s$
$\alpha_7 = \lambda_p P_{\text{suc}} + \mu_s$.

The first equation in (17) represents the normalization equation that should satisfy a Markov Chain. The ten others represent the flow balance at each state, with the $\pi_{(i,j)}, (i,j) \in \{(0,0), \ldots, (n,m)\}$ being the steady probabilities of states $(\text{PU}_0, \text{SU}_0), \ldots, (\text{PU}_n, \text{SU}_m)$. Denoting by $\pi = [\pi_{(0,0)}, \ldots, \pi_{(0,m)}, \ldots, \pi_{(n,0)}, \ldots, \pi_{(n,m)}]$.

The row vector with elements $\pi_{(i,j)}$, the previous equations system can be rewritten as $X\pi = Y$, and with $Y = (1, 0, \ldots, 0)^T$. Matrix X is defined in (18), shown at the top of the page. Hence, $\pi = X^{-1}Y$.

The entries in each row of the matrix X in (18) represent the probabilities for different PUs and SUs. Such a square array is called the matrix of transition probabilities or the transition matrix. Probabilities $\pi_{(i,j)}$ are called transition probabilities. An initial probability distribution, defined on π, specifies the starting state. Usually, this is done by specifying a particular state as the starting state.

Let us adopt the notation $W_k = 2^k CW_{\min}$, where $k \in (0, u)$ is referred to as "backoff stage." u denotes the maximum backoff stage. m denotes the contending numbers of SUs. The probability that a transmitted packet collides by p. The probability τ that a given SU transmits in a randomly selected slot time can now be expressed as [32]

$$\tau = \frac{(1-p)(1-(\frac{p}{1-p})^{u+1})}{1-2p} \cdot \frac{2}{\sum_{k=0}^{u}(\frac{p}{1-p})^k(\text{INT}(CW_{\min})+W_{k-1}+1)}. \tag{19}$$

In the stationary state, each station transmits a packet with probability τ. Therefore, we obtain $p = 1 - (1-\tau)^{m-1}$.

Let P_{tr} be the probability that there is at least one transmission in the considered slot time. Further, let P_s be the probability that a transmission occurring on the channel is successful is given by the probability that exactly one station transmit on the channel, conditioned on the fact that at least one station transmit, given the probability P_{tr} [32]. Therefore, we obtain $p_{tr} = 1 - (1-\tau)^m$, $p_s = \frac{m\tau(1-\tau)^{m-1}}{p_{tr}} = \frac{m\tau(1-\tau)^{m-1}}{1-(1-\tau)^m}$, $p_{\text{idle}} = 1 - p_{tr} = (1-\tau)^m$, $p_{\text{succ}} = p_{tr}p_s = m\tau(1-\tau)^{m-1}$, and $p_{\text{coll}} = 1 - p_{\text{idle}} - p_{\text{succ}} = 1 - (1-\tau)^m - m\tau(1-\tau)^{m-1}$.

Let p_{idle}, p_{succ}, and p_{coll} as the probability that the channel is idle, the probability that a node successfully transmits an RTS packet, and the probability that the collision occurs, respectively.

For GMAC, each SU has two transceiver. Now, we are able to express the average time that is required for the successful handshakes of RTS/CTS/CAS/CAC of GMAC, which can be derived as follows:

$$E[T] = \frac{P_{\text{idle}}T_{\text{ms}} + P_{\text{succ}}T_s + P_{\text{coll}}T_c}{P_{\text{succ}}}. \tag{20}$$

Let T_s and T_c be the average time in the GMAC access scheme in which the channel is sensed busy because of a successful transmission or a collision, and T_{ms} is the mini-slot time units in query window. For the GMAC access scheme, we obtain $T_s = (\text{RTS} + \text{CTS} + \text{CAS} + \text{CAC})/R_{\text{control}} + 4 \times \text{SIFS} + \text{DIFS}$, and $T_c = \frac{\text{RTS}}{R_{\text{control}}} + \text{DIFS}$. Here, RTS, CTS, CAS, and CAC are the time spent by sending a RTS, CTS, CAS, and CAC packet, respectively. SIFS is the time interval of SIFS, and DIFS is the time interval DIFS.

ACKNOWLEDGMENT

The authors would like to thank the editor and the reviewers for their valuable comments and suggestions.

REFERENCES

[1] I. F. Akyildiz, W. Y. Lee, M. C. Vuran, and S. Mohanty, "NeXt generation/dynamic spectrum access/cognitive radio wireless networks: A survey," *Comput. Netw.*, vol. 50, no. 13, pp. 2127–2159, Sep. 2006.
[2] J. Xiang, Y. Zhang, and T. Skeie, "Medium access control protocols in cognitive radio networks," *Wireless Commun. Mobile Comput.*, vol. 10, no. 1, pp. 31–49, Nov. 2010.
[3] C. Cormio and K. R. Chowdhury, "A survey on MAC protocols for cognitive radio networks," *Ad Hoc Netw.*, vol. 7, no. 7, pp. 1315–1329, Sep. 2009.
[4] I. F. Akyildiz, B. F. Lo, and R. Balakrishnan, "Cooperative spectrum sensing in cognitive radio networks: A survey," *Phys. Commun.*, vol. 4, no. 1, pp. 40–62, Mar. 2011.
[5] A. S. Cacciapuoti, M. C. Caleffi, and L. Paura, "Optimal strategy design for enabling the coexistence of heterogeneous networks in TV white space," *IEEE Trans. Veh. Technol.*, vol. 65, no. 9, pp. 7361–7373, Sep. 2016.
[6] M. Caleffi and A. S. Cacciapuoti, "Optimal data access for TV white space," *IEEE Trans. Commun.*, vol. 64, no. 1, pp. 83–93, Jan. 2016.
[7] FCC, "ET docket 10-174: Second memorandum opinion and order in the matter of unlicensed operation in the TV broadcast bands" Active Regulation, Washington, DC, USA: Federal Commun. Commission, Sep. 2012.
[8] Ofcom, "Regulatory requirements for white space devices in the UHF TV band," Ofcom, Active Regulation, London, U.K., Jul. 2012.

[9] *Working Group on Wireless Regional Area Networks, Part 22: Cognitive Wireless RAN Medium Access Control (MAC) and Physical Layer (PHY) Specifications: Policies and Procedures for Operation in the TV Bands*, IEEE 802.22, Active Std., Jul. 2011.
[10] *Wireless Local Area Network Working Group, 802.11af-2013: Part 11: Wireless LAN Medium Access Control (MAC) and Physical Layer (PHY) Specifications Amendment 5: Television White Spaces (TVWS) Operation*, IEEE 802.11af-2013, Active Std., Dec. 2013.
[11] Y. Han, E. Ekici, H. Kremo, and O. Altintas, "A survey of MAC issues for TV white space access," *Ad Hoc Netw.*, vol. 27, no. C, pp. 195–218, Apr. 2015.
[12] S. L. Wu, C. Y. Lin, Y. C. Tseng, and J. P. Sheu, "A new multi-channel MAC protocol with on-demand channel assignment for multi-hop mobile ad hoc networks," in *Proc. Int. Symp. Parallel Archit., Algorithms Netw.*, Dallas, TX, USA, Dec. 2000, pp. 232–237.
[13] J. Jia, Q. Zhang, and X. Shen, "HC-MAC: A hardware-constrained cognitive MAC for efficient spectrum management," *IEEE J. Sel. Areas Commun.*, vol. 7, no. 1, pp. 106–117, Jan. 2008.
[14] Q. Zhao, L. Tong, A. Swami, and Y. Chen, "Decentralized cognitive MAC for opportunistic spectrum access in ad hoc networks: A POMDP framework," *IEEE J. Sel. Areas Commun.*, vol. 25, no. 3, pp. 589–600, Apr. 2007.
[15] B. Hamdaoui and K. G. Shin, "OS-MAC: An efficient MAC protocol for spectrum-agile wireless networks," *IEEE Trans. Mobile Comput.*, vol. 7, no. 8, pp. 915–30, Jun. 2008.
[16] C. Cordeiro and K. Challapali, "C-MAC: A cognitive MAC protocol for multi-channel wireless networks," in *Proc. 2nd IEEE Int. Symp. New Frontiers Dyn. Spectrum Access Netw.*, Dublin, Ireland, Apr. 2007, pp. 147–157.
[17] H. Su and X. Zhang, "CREAM-MAC: An efficient cognitive radio enabled multi-channel MAC protocol for wireless networks," in *Proc. Int. Symp. World Wireless, Mobile Multimedia Netw.*, Newport Beach, CA, USA, Jun. 2008, pp. 1–8.
[18] L. Le and E. Hossain, "OSA-MAC: A MAC protocol for opportunistic spectrum access in congnitive radio networks," in *Proc. IEEE IEEE Wireless Commun. Netw. Conf.*, Las Vegas, NV, USA, Apr. 2008, pp. 1426–1430.
[19] W. S. Jeon, J. A. Han, and D. G. Jeong, "A novel MAC scheme for multichannel cognitive radio ad hoc networs," *IEEE Trans. Mobile Comput.*, vol. 11, no. 6, pp. 922–934, Jun. 2012.
[20] M. Timmers, S. Pollin, A. Dejonghe, L. V. Perre, and F. Catthoor, "A distributed multichannel MAC protocol for multihop cognitive radio networks," *IEEE Trans. Veh. Technol.*, vol. 59, no. 1, pp. 446–459, Aug. 2009.
[21] M. D. Felice, A. J. Ghandhour, H. Artail, and L. Bononi, "Integrating spectrum database and cooperative sensing for cognitive vehicular networks," in *Proc. IEEE VTC Fall*, Las Vegas, NV, USA, Sep. 2013, pp. 1–7.
[22] J. So and N. Vaidya, "Multi-channel MAC for ad hoc networks: Handling multi-channel hidden terminals using a single Transceiver," in *Proc. 5th ACM Int. Symp. Mobile Ad Hoc Netw. Comput.*, New York, NY, USA, May 2004, pp. 222–233.
[23] P. Venkateswaran, S. Shaw, S. Pattanayak, and R. Nandi, "Cognitive radio ad-hoc networks: some new results on multi-channel hidden terminal problem," *Comput. Netw.*, vol. 4, no. 4, pp. 342–348, Nov. 2012.
[24] H. P. Ngallemo, W. Ajib, and H. Elbiaze, "Dynamic spectrum access analysis in a multi-user cognitive radio network using Markov chains," in *Proc. Int. Conf. Comput., Netw. Commun.*, Jan. 2012, pp. 1113–1117.
[25] H. Su and X. Zhang, "Cross-layer based opportunistic MAC protocols for QoS provisionings over cognitive radio wireless networks," *IEEE J. Sel. Areas Commun.*, vol. 26, no. 1, pp. 118–129, Jan. 2008.
[26] P. Ren, Y. Wang, Q. Du and J. Xu, "A survey on dynamic spectrum access protocols for distributed cognitive wireless networks," *EURASIP J. Wireless Commun. Netw.*, vol. 60, pp. 1–21, Dec. 2012.
[27] T. S. Rappaport, *Wireless Communications: Principles and Practice*. Englewood Cliffs, NJ, USA: Prentice-Hall, 1996.
[28] T. Abbas, K. Sjberg, J. Karedal, and F. Tufvesson, "A measurement based shadow fading model for vehicle-to-vehicle network simulations," *Int. J. Antennas Propag.*, vol. 2015, pp. 1–12, Dec. 2015.
[29] S. Merkel, S. Mostaghim, and H. Schmeck, "Distributed geometric distance estimation in ad-hoc networks," in *Proc. 11th Int. Conf. Ad-hoc, Mobile, Wireless Netw.*, Belgrade, Serbia, Jul. 2012, pp. 28–41.
[30] L. T. Tan and L. B. Le, "Fair channel allocation and access design for cognitive Ad Hoc networks," in *Proc. IEEE GLOBECOM*, Anaheim, CA, USA, Dec. 2012, pp. 1162–1167.
[31] L. T. Tan and L. B. Le, "Channel assignment for throughput maximization in cognitive radio networks," in *Proc. IEEE Wireless Commun. Netw. Conf.*, Paris, France, Apr. 2012, pp. 1427–1431.
[32] G. Bianchi, "Performance analysis of the IEEE 802.11 distributed coordination function," *IEEE J. Sel. Areas Commun.*, vol. 18, no. 3, pp. 535–547, Mar. 2000.

Chien-Min Wu was born in Yunlin, Taiwan, in 1966. He received the B.S. degree in automatic control engineering from Feng Chia University, Taichung, Taiwan, in 1989, the M.S. degree in electrical and information engineering from Yuan Ze University, Taoyuan City, Taiwan, in 1994, and the Ph.D. degree from the Department of Electrical Engineering, National Chung Cheng University, Chiayi, Taiwan, in 2004.

In July 1994, he joined the Technical Development Department, Philips Ltd. Co., where he was a Member of the Technical Staff. He is currently an Associate Professor with the Department of Computer Science and Information Engineering, Nanhua University, Chiayi, Taiwan. His current research interests include cognitive radio networks, *ad hoc* networks, and MAC protocol design.

Chih-Pin Lo was born in Taoyuan, Taiwan, in 1992. He received the B.S. degree in computer science and information engineering from the Nanhua University, Chiayi, Taiwan, in 2016. He is currently working toward the M.S. degree in computer science and information engineering at National Chung Cheng University, Chiayi, Taiwan.

His current research interests include *ad hoc* wireless network protocol design.